

Counterfactual Reasoning with Probabilistic Graphical Models for Analyzing Socioecological Systems

Rafael Cabañas^{1*}, Ana D. Maldonado¹, María Morales^{1,3},
Pedro A. Aguilera², Antonio Salmerón^{1,3}

¹Department of Mathematics, University of Almería, Ctra. Sacramento s/n, 04120 La Cañada, Almería, Spain.

²Department of Biology and Geology, University of Almería, Ctra. Sacramento s/n, 04120 La Cañada, Almería, Spain.

³Center for the Development and Transfer of Mathematical Research to Industry (CDTIME), University of Almería, Ctra. Sacramento s/n, 04120 La Cañada, Almería, Spain.

*Corresponding author(s). E-mail(s): rcabanas@ual.es;

Contributing authors: ana.d.maldonado@ual.es; maria.morales@ual.es;
aguilera@ual.es; antonio.salmeron@ual.es;

Abstract

Causal and counterfactual reasoning are emerging directions in data science that allow us to reason about hypothetical scenarios. This is particularly useful in domains where experimental data are usually not available. In the context of environmental and ecological sciences, causality enables us, for example, to predict how an ecosystem would respond to hypothetical interventions. A structural causal model is a class of probabilistic graphical models for causality, which, due to its intuitive nature, can be easily understood by experts in multiple fields. However, certain queries, called unidentifiable, cannot be calculated in an exact and precise manner. This paper proposes applying a novel and recent technique for bounding unidentifiable queries within the domain of socioecological systems. Our findings indicate that traditional statistical analysis, including probabilistic graphical models, can identify the influence between variables. However, such methods do not offer insights into the nature of the relationship, specifically whether it involves necessity or sufficiency. This is where counterfactual reasoning becomes valuable.

Keywords: Causality, Probabilistic graphical models, Structural causal models, Counterfactual reasoning, Socioecological systems

1 Introduction

Causal (and counterfactual) reasoning (Pearl, 2009) allows to analyze cause-effect relationships, which is of fundamental importance for environmental and ecological practitioners and scientists. It can help in the development of effective strategies to mitigate or adapt to environmental problems, such as designing policies to reduce greenhouse gas emissions. This kind of reasoning can also help to evaluate the impact of different human activities on ecosystems.

Causal reasoning can be typically carried out through randomized experiments (a.k.a. randomized control trials), in which the variables of interest are intervened. In doing so, a study sample is divided into one group that will receive the intervention with a given value and another that will be intervened with an alternative value. For example, in the problem of determining if a drug has a significant impact on the recovery from an illness, a group of patients will receive such drug whereas the other will receive a placebo. However, doing a randomized experiment in the field of environmental and ecological sciences might be expensive, unethical or directly impossible. For instance, if we aim to determine the influence of a population (from a specific species) on the structure of an ecosystem, it cannot be removed from it (or introduced in a new one where the population was not originally present). As a consequence, the environmental and ecological data available is usually observational, obtained from non-experimental studies. Using observational data with traditional statistics methods might lead to misleading conclusions when it comes to studying cause-effect relationships.

To illustrate the aforementioned problem, let us consider the observational data from a study (Maldonado et al, 2018), which analyzes the relationship between socioeconomic factors and ecosystem services in cultural landscapes. In particular, the data-set contains information from multiple municipalities in Andalusia (Spain). In this illustrative example, only three Boolean variables are considered: *Mountain* (M) indicating whether the topography is mountainous; *Immigration* (I) indicating if there are more people coming into the area than leaving it; and finally *Agricultural-land* (A) indicating if the land is mainly used for agricultural activities. This data is summarized in Table 1.

From the data presented in the table, it might be possible to build the (discrete) *Bayesian network* (BN) (Pearl, 1988) shown in Fig. 1, which is a popular class of *probabilistic graphical model* (PGM) for doing reasoning under uncertainty. Formally, a BN is a pair consisting of a directed acyclic graph where each vertex corresponds to a random variable, and a set of conditional probability distributions, one for each variable conditional on its parents in the graph. If all the variables are discrete, the conditional distributions are represented as tables, and we will refer to them as CPTs (conditional probability tables).

Table 1: Data from an observational study involving three Boolean variables (Maldonado et al, 2018).

Mountain (M)	Immigration (I)	Agricultural-land (A)	Counts
yes	yes	yes	95
yes	yes	no	244
yes	no	yes	80
yes	no	no	183
no	yes	yes	121
no	yes	no	52
no	no	yes	47
no	no	no	8

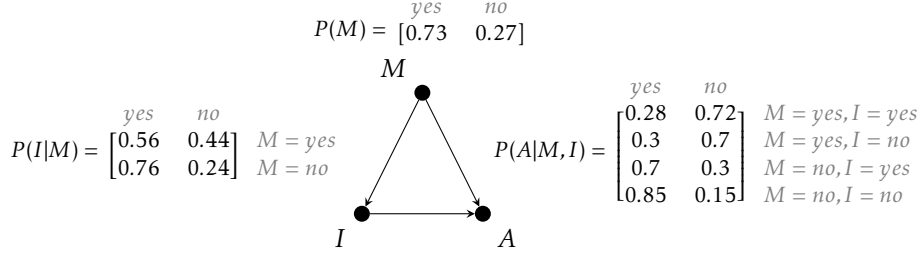


Fig. 1: BN obtained from the observational data in Table 1.

When studying the impact of immigration on the land use, one might consider to analyze the distribution $P(A|I) = \sum_M P(A|I, M) \cdot P(I|M) \cdot P(M)$. From the CPTs in Fig. 1, it follows that $P(A = \text{yes}|I = \text{yes}) = 0.42$ and $P(A = \text{yes}|I = \text{no}) = 0.39$. As there is a positive correlation between both variables, one could conclude that immigration has a positive effect on agriculture. However, analyzing separately the data in mountainous and flat areas, the correlation is the opposite as we have: $P(A = \text{yes}|M = \text{yes}, I = \text{yes}) < P(A = \text{yes}|M = \text{yes}, I = \text{no})$ and $P(A = \text{yes}|M = \text{no}, I = \text{yes}) < P(A = \text{yes}|M = \text{no}, I = \text{no})$. This is an instance of the so-called Simpson's Paradox (see, for example, (Pearl, 2009, Ch.6)), which refers to a phenomenon whereby the association between a pair of variables reverses sign upon conditioning on a third variable (a confounder): flat areas are more likely to have immigration and also this topography is more suitable for an agricultural use of the land. A further explanation for this paradoxical situation, is that it is not the same seeing than doing. When calculating $P(A|I = \text{yes})$, we are essentially asking about the probability of the agricultural land use *given that we see* that there is immigration. However, we might be interested in determining if the immigration is a necessary condition for the agricultural land use. In other words, if immigration were to cease in a given area, would it lead to a reduction in agricultural land use? Conversely, it is also valuable to understand if promoting immigration would be advantageous for agriculture, in which case we say that it is sufficient condition. These scenarios involve hypothetical situations that can be effectively addressed through counterfactual reasoning.

In line with the previous illustrative example, this paper aims to study the influence of socio-economy on land uses and population growth, in the conceptual framework of socio-ecological systems (Anderies et al, 2004). Socio-ecological systems encompass the intricate interplay between human systems and natural ecosystems (Berkes et al, 2003; Preise et al, 2018). The socio-ecological system is a complex adaptive system, with some properties, such as as: non-linear dynamics, critical thresholds, tipping points, regime shifts (Scheffer et al, 2012; Hughes et al, 2013; Mathias et al, 2020; Arnaiz-Schmitz et al, 2023), system memory, cross-scale linkages (Parrott and Quinn, 2016) and uncertainty (Biggs et al, 2015). Due to their properties, the tools for modeling these systems should consider the uncertainty. In the socio-ecological context, land-use changes (integrated in a landscape) are primarily driven by socio-economic processes, influencing the ecological integrity of these landscapes, therefore changes in socio-economic structures and processes induce an alteration of the landscapes (Schmitz et al, 2003).

In this paper, we provide a coherent overview of the fundamental concepts for applying causal and counterfactual reasoning to data analysis within the domain of environmental and ecological sciences. In particular, we consider the use of *structural causal models* (SCM) (Pearl, 2009; Bareinboim et al, 2022), a class of PGM for counterfactual reasoning. Like most of the PGMs, these are suitable for environmental and ecological scientists and practitioners due to the intuitive nature of PGMs. Moreover, the recent method *expectation-maximization for causal computation* (EMCC) (Zaffalon et al, 2023b,a) is proposed to be used for counterfactual reasoning. A key advantage of this method is its ease of implementation, primarily built upon the widely recognized *expectation-maximization* (EM) (Koller and Friedman, 2009, Ch.19) approach for parameter learning in PGMs. We put these concepts into practical use with an observational data-set including information about socioeconomic factors and the land uses (e.g., crops, building, natural, etc.) in different areas of Andalusia (southern Spain). Unlike traditional analysis with other PGMs, the use of SCMs allows to analyze the relations of necessity and sufficiency between the variables in the aforementioned socio-ecological system.

This paper is structured as follows. Section 2 reviews the relevant literature regarding the use of PGMs in the analysis of environmental data; Section 3 introduces the fundamentals of causal and counterfactual reasoning, with a specific focus on SCMs; Section 4 provides details about the case of study considered for counterfactual analysis; the analysis of the results is presented in Section 5; finally, Section 6 offers an overview of the main conclusions drawn from this paper.

2 Related work

Causal modeling techniques have been used in Environmental sciences in a wide range of works. Paul (2011) highlights the simplicity and effectiveness of causal modeling approach at dealing with confounding, in comparison to the broadly accepted before-after control-impact designs. Later, Paul and Anderson (2013) proposed ordination axes arising from multivariate macrobiotic species data in conjunction with structural equation modeling (SEM) approach to analyze the impact of the 1978

Amoco Cadiz oil spill. In this work, the conditional independencies are considered by the authors as the only means to test causal structures with observational data (Paul and Anderson, 2013). SEM are also used in (Paul et al, 2016) to assess the risk of wastewater discharge on macro-invertebrate communities, focusing in the adaptation of the causal diagram to a statistical model which allows for computing the effect of an intervention retrospectively.

Structural equation modeling and Bayesian networks (BNs) have proven to be useful tools to control spatiotemporal confounding in environmental studies (Hatami, 2019, 2018a,b). Another work (Hatami, 2018a) integrates BNs with SEM to infer causal effects of wastewater on the macro-invertebrate community once the effect of natural variation is removed or to analyse the spatiotemporal variations of macrobenthic assemblage caused by leaking from a wastewater treatment plant.

Another common issue in environmental studies which is addressed by SEM is multicollinearity: Bizzi et al (2013) use SEM framework in the study of the relationships between water quality, physical habitat and benthic macroinvertebrate community in rivers, finding that SEM reduce errors due to multicollinearity thanks to the a priori selection of variables and paths. Ramazi et al (2021) use BNs to deal with missing values and highly correlated covariates in their study of a mountain pine beetle infestation. Irvine et al (2015) combine Bayesian path analysis and SEM to study the effect of stressors (such as anthropogenic drivers of road density, percent grazing or percent forest within a catchment) affect stream biological condition.

Carriger et al (2016) recommend the use of BNs for evidence-based policy in environmental management, on the grounds that these graphical models can look into the evidence for causality through improved measurements, minimizing biases in predicting or diagnosing causal relationships. In their review, the authors propose several guidance works on BN development for environmental problems and, as practical example, use BNs to study the impacts of biological and chemical stressors on a fish population.

Nyberg et al (2006) discuss the applications of BNs to adaptive-management processes, by illustrating the system relations, calculating joint probabilities for decision options or predicting the outcomes of management policies. They exemplify the use of BNs in an adaptive management of forest and terrestrial lichens.

Influence Diagrams (IDs) are probabilistic networks that extend the BN by including information about the interactions of decisions with the system. Carriger et al (Carriger and Barron, 2011) develop an ID for the Deepwater Horizon spill event, which is used to display the impacts of decisions and spilled oil on ecological variables and services. This modeling framework is proposed for assistance in future responses to oil spills because it points out important variables and relationships to be accounted for by decision makers to get a better understanding of the potential outcomes. Carriger and Newman (2012) also propose IDs for causal inference in ecological risk-based management of pesticide usage.

Besides causal modeling, counterfactual thinking is essential in environmental policy to draw inferences about program effectiveness as well as to discriminate between program effect and biases (Ferraro, 2009). Andam et al (2008) apply counterfactual thinking by using matching methods to improve the estimate of the

impact of protected areas in Costa Rica on deforestation. In that work, the authors demonstrate that counterfactual thinking let control biases along observable features and check the sensitivity of the estimates to potential hidden biases. Also a statistical matching technique is used by [McConnachie et al \(2016\)](#) to estimate cost-effectiveness of South Africa’s Working for Water program on reducing invasive species.

In relation to our case of study, various methodologies have been employed, including multiple regression ([De Aranzabal et al, 2008](#)), econometric models ([Punzo et al, 2022](#)), graphical spatial models ([Irvine and Gitelman, 2011](#)), panel-data co-integration techniques ([Subramaniam et al, 2023](#)), and BNs ([Roperio et al, 2019](#)). However, to the best of our knowledge, counterfactual reasoning with PGMs has not yet been explored in the context of socio-ecological systems. This approach could offer a new dimension to the study of socio-economic influences on land use changes within socioecological systems.

3 Background and notation

This section provides an overview of fundamental concepts related to PGMs for causal and counterfactual reasoning. It is advisable for the reader to have a familiarity with PGMs, especially discrete BNs. If the reader is not already acquainted with these concepts, they can refer to ([Pearl, 1988](#); [Jensen and Nielsen, 2007](#); [Koller and Friedman, 2009](#)) for a more in-depth understanding.

With respect to the general notation, upper-case letters are used to denote random variables and lower-case for their possible values (or states). That is, given a variable V , v is an element of its domain, denoted by Ω_V . We assume that all the variables are discrete. Similarly, $\mathbf{V} = \{V_1, V_2, \dots, V_n\}$ denotes a set of variables and \mathbf{v} a joint state of its domain $\Omega_{\mathbf{V}} = \times_{V \in \mathbf{V}} \Omega_V$. For the sake of simplicity, variables are omitted from assignments when their context is clear. For instance, $P(V = v)$ will be denoted simply as $P(v)$.

3.1 Structural causal models

Structural causal models (SCMs) ([Pearl, 2009](#)) are a specific type of probabilistic graphical model used for causal and counterfactual reasoning. In essence, SCMs extend BNs by distinguishing between two types of nodes: *endogenous* nodes, which represent the variables within the modeled problem, and *exogenous* nodes, which are associated with external factors. Note that the terms node and variable are used interchangeably. SCMs can be formally defined as follows ([Bareinboim et al, 2022](#)).

Definition 1 (Structural causal model (SCM)). *A structural causal model \mathcal{M} is a 5-tuple $\langle \mathbf{U}, \mathbf{X}, \mathcal{G}, \mathcal{F}, \mathcal{P} \rangle$, where*

- \mathbf{U} is a set of exogenous variables that are determined by factors outside the model;
- \mathbf{X} is a set of variables $\{X_1, X_2, \dots, X_n\}$, called endogenous, that are determined by other variables in the model i.e., variables in $\mathbf{U} \cup \mathbf{X}$.
- \mathcal{G} is a directed acyclic graph (DAG), called the causal graph of the model, whose nodes are the variables $\mathbf{U} \cup \mathbf{X}$.

- \mathcal{F} is a set of functions $f_{X_1}, f_{X_2}, \dots, f_{X_n}$ called *structural equations (SE)*, such that each of them is a map $f_X : \Omega_{\text{Pa}_X} \rightarrow \Omega_X$, where Pa_X are the parents (i.e., the immediate predecessors) of X according to \mathcal{G} .
- \mathcal{P} is a set containing a probability distribution $P(U)$ for each $U \in \mathbf{U}$.

As an illustrative example, we will begin by examining Fig. 2, which depicts two potential causal graphs for SCMs extending the BN presented in Fig. 1. The endogenous variables, represented as black nodes, correspond to the variables originally found in the initial BN, specifically $\mathbf{X} = \{M, I, A\}$. These variables retain their original domains. In addition to the endogenous variables, the causal graphs also incorporate exogenous variables, which are depicted as gray nodes. In the left graph, the set of exogenous variables is $\mathbf{U} = \{U, V, W\}$, while in the right graph, it is $\mathbf{U} = \{U, W\}$.

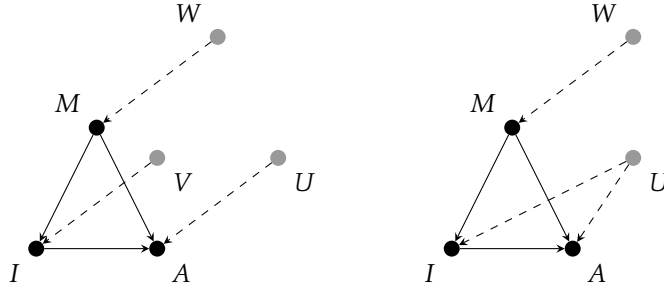


Fig. 2: Examples of two possible causal graphs for the problem shown in Fig. 1.

The distinction between the two causal graphs is as follows: the graph on the left assumes the absence of any exogenous (and hidden) confounder between any pair of variables. In contrast, in the graph on the right, variables I and A are both influenced by the exogenous variable U . According to the classification in (Avin et al, 2005), an SCM with a graph like the one on the left is termed *Markovian*, signifying that each exogenous variable has only one endogenous child. Conversely, an SCM with a graph like the one on the right is termed *semi-Markovian*, indicating that any of the exogenous variables can have more than one endogenous child¹. It's important to note that in both cases, all endogenous variables must have exactly one exogenous parent. In other words, given the endogenous variables, each exogenous variable is independent of the other ones, i.e., it holds that $U_i \perp\!\!\!\perp U_j | \mathbf{X}$ for all $U_i, U_j \in \mathbf{U} \times \mathbf{U}$ with $i \neq j$. If this condition is not satisfied the model will be classified as *non-Markovian*.

A parametrization for the previously mentioned SCM is illustrated in Fig. 3. The set of marginal distributions associated with the exogenous variables is $\mathcal{P} = \{P(U), P(V), P(W)\}$. Conversely, the set of SEs is represented by $\mathcal{F} = \{f_A(U, I, M), f_I(V, M), f_M(W)\}$. It is worth noting that each SE $f_X(\text{Pa}_X)$ induces a degenerate CPT of the form $P(X|\text{Pa}_X)$, characterized by containing only ones and zeros. This underscores the connection with BNs: an SCM can be viewed as a BN

¹Some authors consider a less general definition and limit exogenous variables in semi-Markovian models to have no more than 2 variables (Huang and Valtorta, 2006).

subject to certain constraints in both the DAG and the type of CPTs it employs. For simplicity, the notation in form of CPT will be mainly used. For instance, the SE for M , which is shown below, corresponds to the CPT $P(M|W)$ in Fig. 3.

$$f_M(W) = \begin{cases} yes & \text{if } W = w_1, \\ no & \text{if } W = w_2. \end{cases}$$

$$P(W) = \begin{matrix} w_1 & w_2 \\ [0.7253 & 0.2747] \end{matrix} \quad P(V) = \begin{matrix} v_1 & v_2 & v_3 & v_4 \\ [0.56312 & 0 & 0.19565 & 0.24123] \end{matrix}$$

$$P(U) = \begin{matrix} u_1 & u_2 & u_3 & u_4 & u_5 & u_6 & u_7 & u_8 & u_9 & u_{10} \\ [0 & 0.24979 & 0 & 0 & 0.03045 & 0.30418 & 0 & 0.14545 & 0 & 0.27013] \end{matrix}$$

$$P(M|W) = \begin{matrix} w_1 & w_2 \\ \begin{bmatrix} 1 & 0 \\ 0 & 1 \end{bmatrix} \end{matrix} \begin{matrix} M = yes \\ M = no \end{matrix} \quad P(I|M, V) = \begin{matrix} v_1 & v_2 & v_3 & v_4 \\ \begin{bmatrix} 1 & 1 & 0 & 0 \\ 0 & 0 & 1 & 1 \\ 1 & 0 & 1 & 0 \\ 0 & 1 & 0 & 1 \end{bmatrix} \end{matrix} \begin{matrix} M = yes, I = yes \\ M = yes, I = no \\ M = no, I = yes \\ M = no, I = no \end{matrix}$$

$$P(A|M, I, U) = \begin{matrix} u_1 & u_2 & u_3 & u_4 & u_5 & u_6 & u_7 & u_8 & u_9 & u_{10} \\ \begin{bmatrix} 1 & 1 & 1 & 1 & 1 & 0 & 0 & 0 & 0 & 0 \\ 0 & 0 & 0 & 0 & 0 & 1 & 1 & 1 & 1 & 1 \\ 1 & 0 & 1 & 1 & 0 & 1 & 0 & 0 & 1 & 0 \\ 0 & 1 & 0 & 0 & 1 & 0 & 1 & 1 & 0 & 1 \\ 1 & 1 & 0 & 0 & 0 & 1 & 1 & 1 & 0 & 0 \\ 0 & 0 & 1 & 1 & 1 & 0 & 0 & 0 & 1 & 1 \\ 1 & 1 & 1 & 0 & 1 & 1 & 1 & 0 & 1 & 1 \\ 0 & 0 & 0 & 1 & 0 & 0 & 0 & 1 & 0 & 0 \end{bmatrix} \end{matrix} \begin{matrix} M = yes, I = yes, A = yes \\ M = yes, I = yes, A = no \\ M = yes, I = no, A = yes \\ M = yes, I = no, A = no \\ M = no, I = yes, A = yes \\ M = no, I = yes, A = no \\ M = no, I = no, A = yes \\ M = no, I = no, A = no \end{matrix}$$

Fig. 3: SEs and marginal distributions for the Markovian SCM in Fig. 2 (left). Note that the SEs are represented as CPTs.

In the formalism of SCMs, SEs are typically assumed to be provided, often derived from expert knowledge. Alternatively, SEs can be automatically inferred from the causal graph, without any loss of generality, via *canonical specification*. The states of an exogenous variable will then represent all possible mechanisms between its children and their respective endogenous parents. This requires that the exogenous variables have a specific number of states, as determined by Theorem 1. In Fig. 3, the SEs associated to variables M and I are already canonical, whereas the one for A is not. The SE under the canonical specification for A and the corresponding distribution $P(U)$ are shown in Fig. 4.

Theorem 1 (Pearl (2009)). *Let U be an exogenous variable, let \mathbf{V} be its endogenous children and let \mathbf{Y} be the endogenous parents of \mathbf{V} and which are not already present in \mathbf{V} . Then U requires $|\Omega_{\mathbf{V}}|^{|\Omega_{\mathbf{Y}}|}$ states for a canonical specification.*

$$P(U) = \begin{bmatrix} u_1 & u_2 & u_3 & u_4 & u_5 & u_6 & u_7 & u_8 & u_9 & u_{10} & u_{11} & u_{12} & u_{13} & u_{14} & u_{15} & u_{16} \\ 0 & 0 & 0 & 0 & 0.16 & 0.12 & 0 & 0 & 0 & 0 & 0.02 & 0.68 & 0 & 0 & 0 & 0.02 \end{bmatrix}$$

$$P(A|M, I, U) =$$

u_1	u_2	u_3	u_4	u_5	u_6	u_7	u_8	u_9	u_{10}	u_{11}	u_{12}	u_{13}	u_{14}	u_{15}	u_{16}	
1	1	1	1	1	1	1	1	0	0	0	0	0	0	0	0	$M = \text{yes}, I = \text{yes}, A = \text{yes}$
0	0	0	0	0	0	0	0	1	1	1	1	1	1	1	1	$M = \text{yes}, I = \text{yes}, A = \text{no}$
1	1	0	0	1	1	0	0	1	1	0	0	1	1	0	0	$M = \text{yes}, I = \text{no}, A = \text{yes}$
0	0	1	1	0	0	1	1	0	0	1	1	0	0	1	1	$M = \text{yes}, I = \text{no}, A = \text{no}$
1	1	1	1	0	0	0	0	1	1	1	1	0	0	0	0	$M = \text{no}, I = \text{yes}, A = \text{yes}$
0	0	0	0	1	1	1	1	0	0	0	0	1	1	1	1	$M = \text{no}, I = \text{yes}, A = \text{no}$
1	0	1	0	1	0	1	0	1	0	1	0	1	0	1	0	$M = \text{no}, I = \text{no}, A = \text{yes}$
0	1	0	1	0	1	0	1	0	1	0	1	0	1	0	1	$M = \text{no}, I = \text{no}, A = \text{no}$

Fig. 4: Canonical SE for A (represented as a CPT) and marginal distribution for variable U in the Markovian SCM in Fig. 2.

In a Markovian model, Algorithm 1 can be employed to initialize a SE with the canonical specification. In case of confounders, each endogenous variable influenced by confounders can be initialized using an independent exogenous variables. Subsequently, these independent exogenous variables can be replaced with a single variable, where each state of the new exogenous variable corresponds to a joint state of the initially independent ones.

Algorithm 1 Canonical specification in a Markovian model

input: V (endogenous variable associated to the SE), \mathbf{Y} (set of endogenous parents of V), U (exogenous parent of V)
output: $f_V(U, \mathbf{Y})$ (initialized SE)

- 1: $m \leftarrow |\Omega_{\mathbf{Y}}|$
- 2: $\Omega_U \leftarrow \{u_1, u_2, \dots, u_{|\Omega_U|^m}\}$
- 3: $i \leftarrow 1$
- 4: **for** $(v^{(1)}, v^{(2)}, \dots, v^{(m)}) \in \times_{k=1}^m \Omega_V$ **do**
- 5: **for** $k \leftarrow 1, \dots, m$ **do**
- 6: $f_V(u_i, \mathbf{y}_k) \leftarrow v^{(k)}$
- 7: **end for**
- 8: $i \leftarrow i + 1$
- 9: **end for**
- 10: **return** $f_V(U, \mathbf{Y})$

Up to this point, we have assumed that all parameters are readily available, and consequently, models of this nature will be denoted as *fully-specified SCMs*. However, in practice, only data from the endogenous variables is accessible, and hence the exogenous distributions are not available. Models of this kind will be referred to as *partially-specified SCMs*. We will address this issue in Section 3.4. In the subsequent sections covering inference, we will, nonetheless, assume a complete specification of the parameters.

3.2 Probabilistic, causal and counterfactual inference

Typically, performing probabilistic inference in PGMs involves computing the posterior probability distribution for a set of variables of interest given evidence about some other variables. In the BN depicted in Fig. 1, for example, we may be interested in calculating $P(A|I = \text{yes})$, that is, the probability that an area has an agricultural use, given that we observe that there is immigration. This is called *observational* query, which can also be calculated in SCMs. Let X and Y be two endogenous variables, the conditional probability of Y given that we observe X can be calculated as

$$P(Y|X) = \frac{\sum_{\mathbf{U}} \sum_{\mathbf{X} \setminus \{X, Y\}} \prod_{U \in \mathbf{U}} P(U) \prod_{X_i \in \mathbf{X}} P(X_i | Pa_{X_i})}{\sum_{\mathbf{U}} \sum_{\mathbf{X} \setminus \{X\}} \prod_{U \in \mathbf{U}} P(U) \prod_{X_i \in \mathbf{X}} P(X_i | Pa_{X_i})}. \quad (1)$$

As an example, let us consider the SCM with the graph from Fig. 2 (left) and the observational query $P(A|I = \text{yes})$. For this, the joint probability is first calculated (Eq. (2)) and then normalized (Eq. (3)) as follows.

$$\begin{aligned} P(A, I = \text{yes}) &= \sum_{\mathbf{U}} \sum_M P(U)P(V)P(W)P(A|I = \text{yes}, M, U)P(I = \text{yes}|M, V)P(M, W) \\ &= \sum_M P(A|I = \text{yes}, M)P(I = \text{yes}|M)P(M), \end{aligned} \quad (2)$$

$$P(A|I = \text{yes}) = \frac{P(A, I = \text{yes})}{P(A = \text{yes}, I = \text{yes}) + P(A = \text{no}, I = \text{yes})}. \quad (3)$$

As shown in Eq. (2), observational queries in an SCM can be expressed as distributions containing only endogenous variables. As a result, they can be easily computed from observational data. Consequently, such queries may not hold much interest within the context of SCMs. Furthermore, the semantics of these types of queries involve calculating the probability of one event occurring given the observation of another.

On the contrary, causal reasoning often requires us to contemplate hypothetical scenarios. In other words, we are frequently more interested in calculating the probability of a variable given that we intervene on another. This can be achieved with the so-called *do calculus* (Pearl, 2009), which requires to introduce the intervention operator, denoted as $do(\bullet)$. When given an exogenous variable X and $x \in \Omega_X$, the operator $do(x)$ is called an intervention and simulates the action of forcing X to take the specific value x . This operation, often referred to as surgery, is essentially a graphical operation involving the removal of incoming arcs into the intervened variable X and the replacement of its SE with a map $X = x$. The model resulting from this surgery is referred to as the ‘post-intervention’ model, denoted as \mathcal{M}_x . This model can be used for calculating causal queries, as detailed in Theorem 2, i.e.,

the probability of a target variable in a hypothetical scenario where another variable is intervened.

Theorem 2 (Pearl (2009)). Consider two exogenous variables, Y and X , within a SCM, and let x represent a state in the set Ω_X . In this context, the interventional query $P(Y|do(x))$ can be transformed into an observational query within the post-interventional model \mathcal{M}_x , as follows:

$$P(Y|do(x)) = P_{\mathcal{M}_x}(Y|x). \quad (4)$$

In the context of the model under consideration, it may be of interest to calculate the query $P(A|do(I = yes))$, which represents the probability of agricultural land use when immigration is enforced. Such interventional query can be calculated as the observational query $P_{\mathcal{M}_{I=yes}}(A|I = yes)$ in the post-interventional model $\mathcal{M}_{I=yes}$ depicted in Fig. 5 as follows.

$$P(A|do(I = yes)) = \sum_{W,U,M} P(A|I = yes, M, U)P(U)P(M|W)P(W). \quad (5)$$

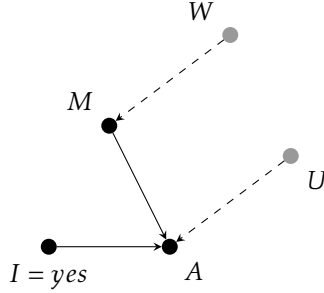


Fig. 5: Post-interventional model $\mathcal{M}_{I=yes}$ resulting of applying the intervention $do(I = yes)$ in the model from Fig. 2 (left).

In a more general setup, counterfactual inference allows scenarios in which the same variable can be both observed and subject to intervention. In essence, it enables reasoning about a hypothetical scenario based on our knowledge of reality. In this context, the counterfactual query $P(Y_x = y|X = x', Y = y')$ represents the probability of event y occurring in a hypothetical scenario where the variable X is intervened to take value x , given that in reality, events x' and y' occurred. The notation $Y_{X=x}$ or simply Y_x denote the variable Y in the hypothetical scenario, whereas variables in the reality remain with the name unchanged. Counterfactual queries can be computed by means of an extended model based on the so-called *counterfactual model*, which can be defined as follows.

Definition 2 (Counterfactual model). A counterfactual model is a SCM including endogenous from both the real and hypothetical scenario, obtained by duplicating the sub-graph composed of the endogenous nodes for the real scenario, and then applying the intervention.

Note that in the counterfactual model, the endogenous nodes in both the real and hypothetical scenarios share the same exogenous parents, with the exception of the intervened variables. As an example, Fig. 6 depicts the counterfactual model for the intervention $do(I = yes)$. Note that this can be extended to any number of scenarios associated with different interventions. As all the variables relevant for a counterfactual query are represented in this extended model, its computation can be done as an observational query consisting in the conditional probability of the target variable given the observed and the intervened variables.

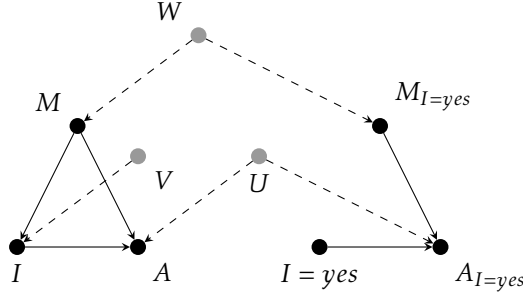


Fig. 6: Counterfactual model involving the reality and the hypothetical scenario under the intervention $do(I = yes)$.

3.3 Standard queries for causal and counterfactual analysis

The use of the counterfactual model defined above, facilitates the specification of a number of typical queries that can be useful for understanding the model but also for defining policies aimed at solving problems in the environment represented by our model. In general, the queries reviewed in this section are related to the abstract concepts of *necessity* (when something must occur in order to something else to happen) and *sufficiency* (when something is enough for something else to take place).

From now on, if x is a possible value of a variable X , we will denote by x' the complement of x . Also, as introduced in Section 3.2, we will denote by $Y_x = y$ the event consisting in variable Y taking value y in a scenario where X is intervened take value x . Note that all of the following queries (i.e. the computation of the following probabilities) are carried out over the counterfactual model (see Definition 2).

Definition 3 (Probability of necessity (Pearl, 2009)). Let X and Y be two variables in an SCM. The probability of necessity is defined as

$$PN(X, Y) = P(Y_{x'} = y' | X = x, Y = y). \quad (6)$$

PN can be interpreted as the probability that Y would not have taken value y if X had not taken value x , given that in fact variables X and Y took values x and y respectively. In other words, it measures to what extent it is necessary that X takes value x for Y to take value y . It might also be useful to consider the probability of necessity, but assuming that $X = x$ did not happen. We call it the *probability of necessity with reverse cause*, formally defined as

Definition 4 (Probability of necessity with reverse cause). *Let X and Y be two variables in an SCM. The probability of necessity with reverse cause is defined as*

$$\text{PNrc}(X, Y) = P(Y_x = y' | X = x', Y = y). \quad (7)$$

The abstract concept of sufficiency is addressed by the following definition, and measures the capacity of X taking value x causing Y to take value y .

Definition 5 (Probability of sufficiency (Pearl, 2009)). *Let X and Y be two variables in an SCM. The probability of sufficiency is defined as*

$$\text{PS}(X, Y) = P(Y_x = y | X = x', Y = y'). \quad (8)$$

The following definition is closely related to PN and PS. It measures how Y reacts to X , hence expressing to what extent $X = x$ is necessary and sufficient for $Y = y$.

Definition 6 (Probability of necessity and sufficiency (Pearl, 2009)). *Let X and Y be two variables in an SCM. The probability of necessity and sufficiency is defined as*

$$\text{PNS}(X, Y) = P(Y_x = y, Y_{x'} = y'). \quad (9)$$

The formal relation between the three probabilities defined above is given by (Pearl, 2009)

$$\text{PNS}(X, Y) = P(X = x, Y = y)\text{PN}(X, Y) + P(X = x', Y = y')\text{PS}(X, Y). \quad (10)$$

The following two queries are particularly useful for policy makers interested in avoiding or making something happen by intervening some controllable variable. This is reflected in the probabilities of *disablement* and *enablement*, which respectively measure the probability that Y changes from y to y' if X is forced to the value x' , and the probability that Y would have taken value y if X had taken value x . They are formally defined as follows.

Definition 7 (Probability of disablement (Pearl, 2009)). *Let X and Y be two variables in an SCM. The probability of disablement is defined as*

$$\text{PD}(X, Y) = P(Y_{x'} = y' | Y = y). \quad (11)$$

Definition 8 (Probability of enablement (Pearl, 2009)). *Let X and Y be two variables in an SCM. The probability of enablement is defined as*

$$\text{PE}(X, Y) = P(Y_x = y | Y = y'). \quad (12)$$

Besides the queries described so far, we will also consider two more queries that are not computed in the counterfactual model, namely the *difference in conditional probability*, $P(y|x) - P(y|x')$, and the *average causal effect*, which is defined as

$$\text{ACE}(X, Y) = P(y_x) - P(y_{x'}). \quad (13)$$

3.4 Unidentifiable queries

As detailed in Section 3.2, having access to exogenous probabilities enables the computation of causal or counterfactual queries using standard inference algorithms for BNs. However, in real-world problems, data from the endogenous variables is typically the only information available. Consequently, quantifying these exogenous probabilities is not feasible. Nevertheless, some queries, known as *identifiable*, can be reduced to an expression that involve only distributions without exogenous variables. In this way, Eq. (5) can be simplified as

$$\begin{aligned} P(A|do(I = yes)) &= \sum_M \sum_U P(A|I = yes, M, U) P(U) \sum_W P(M|W) P(W) \\ &= \sum_M P(A|I = yes, M) P(M). \end{aligned} \quad (14)$$

The process of transforming a query into an expression computable from the endogenous data is elucidated in detail in (Tian and Pearl, 2002). This procedure is specifically applicable to interventional queries that are identifiable. An interventional query is considered identifiable when the exogenous parents of the intervened variables do not have more than one child. Regarding counterfactual queries, recent studies (Correa et al, 2021; Wu et al, 2019) have demonstrated that these queries are identifiable when both observational and interventional data are accessible. However in our specific case study involving environmental data, such interventional data is not available; we only have access to observational data. As a consequence, most of the queries are unidentifiable. In this context, there are a few methods allowing, from only observational data, to bound unidentifiable counterfactual queries. In other words, the results is a probability interval rather than a single value. One approach, presented by Tian and Pearl (2000), offers analytical expressions to compute bounds in specific types of models. Another method, proposed by Zaffalon et al (2020), transforms SCMs into models with imprecise probabilities to address unidentifiable queries. In our specific case study, we adopt an approximate method to bound unidentifiable queries. This method treats the problem as one of learning PGMs with latent variables, and its details are expounded upon in the following section.

3.5 Approximate method for bounding unidentifiable queries

In order compute any causal or counterfactual query, it is required the estimation of probabilities associated with exogenous variables. In this regard, we propose the

utilization of the innovative technique known as EMCC (*Expectation Maximization for Causal Computation*) as detailed in (Zaffalon et al, 2023b,a). An advantageous feature of this approach is its ability to be implemented using inference and learning algorithms designed for BNs with latent variables.

Broadly, this method considers that a SCM can be regarded as a BN in which the exogenous variables are treated as latent. The idea is to repeatedly apply a learning algorithm for BNs with latent variables. Each run of this algorithm generates a fully-specified SCM, from which any query can be calculated and then aggregated to derive the bounds of that query in the partially-defined SCM. In the case of EMCC, the well-known EM algorithm (Koller and Friedman, 2009, Ch.19) is employed. The overall procedure is illustrated in Algorithm 2, which takes as input a partially defined SCM denoted as \mathcal{M} , a data-set of observations from the endogenous variables denoted as \mathcal{D} , and a parameter N , representing the number of independent runs conducted. The output is the set \mathcal{M} containing a total of N SCMs, each of them can have a different specification for the exogenous distributions. Note that, to introduce such diversity in the resulting models, in line 3, the exogenous distributions are randomly sampled, ensuring that each EM execution starts from a different prior model (i.e., starting model). Conversely, the SEs remain unchanged. The prior model for the i_{th} EM run and its exogenous distributions are denoted \mathcal{M}'_i and $\{P'_i(U)\}_{U \in \mathcal{U}}$ respectively. In line 5, the standard version of the EM algorithm is executed, with the advantage that the latent variables act as root nodes, while their children are observed. A specific version of EM tailored for causal reasoning is described in (Zaffalon et al, 2023b,a).

Algorithm 2 Learning with EMCC

input: \mathcal{M} (partially-specified SCMs), \mathcal{D} (endogenous data-set), N (number of runs)

output: $\mathcal{M} = \{\mathcal{M}_1, \mathcal{M}_2, \dots, \mathcal{M}_N\}$ (set of fully-specified SCMs)

```

1:  $\mathcal{M} \leftarrow \emptyset$ 
2: for  $i \in \{1, \dots, N\}$  do
3:    $\{P'_i(U)\}_{U \in \mathcal{U}} \leftarrow$  Random initialization  $\{P(U)\}_{U \in \mathcal{U}}$  from  $\mathcal{M}$ 
4:    $\mathcal{M}'_i \leftarrow$  build a SCM with  $\{P'_i(U)\}_{U \in \mathcal{U}}$ 
5:    $\mathcal{M}_i \leftarrow \text{EM}(\mathcal{M}'_i, \mathcal{D})$ 
6:    $\mathcal{M} \leftarrow \mathcal{M} \cup \{\mathcal{M}_i\}$ 
7: end for
8: return  $\mathcal{M}$ 

```

Once a sufficiently large set of fully-specified SCMs is available, it becomes possible to calculate bounds for any query, whether it's a causal or counterfactual one. For this purpose, the desired query needs to be computed within each model. This procedure is outlined in Algorithm 3, which takes as input a set of fully-specified SCMs denoted as \mathcal{M} , and a causal or counterfactual query denoted as Q . In line 3, the result of calculating such a query in a specific model \mathcal{M} is represented as $Q_{\mathcal{M}}$. Then, output consists of the lower and upper bounds for this query in the original model \mathcal{M} , taking into account the data-set \mathcal{D} . These bounds are determined by finding the

infimum and supremum values across all individual queries. The bounds calculated using EMCC are indeed approximations of the actual bounds. This approximation arises from two primary reasons. First, the number N of fully-specified SCMs may not be sufficiently high to fully encompass the actual interval. Secondly, the individual executions of the EM algorithm might not have converged to a high degree of accuracy, leading to some level of error.

Algorithm 3 Inference

input: \mathcal{M} (set of fully-specified SCMs), Q (causal or counterfactual query)

output: lower and upper bounds of Q

```

1:  $Q \leftarrow \emptyset$ 
2: for  $\mathcal{M} \in \mathcal{M}$  do
3:    $Q \leftarrow Q \cup \{Q_{\mathcal{M}}\}$ 
4: end for
5: return  $(\inf(Q), \sup(Q))$ 

```

For the purpose of illustration, we will use the model and data from our motivational example. In this context, \mathcal{M} is the SCM with the graph displayed in Fig. 2 (left) and the SEs given in Fig. 3 and \mathcal{D} is the data-set described in Table 1. For the sake of simplicity, we will consider $N = 2$, though in a real setting this should take a higher value. Let us consider that the random prior distributions for both executions (line 3 of Algorithm 2) are those shown in Fig. 7.

$$\begin{aligned}
P'_1(W) &= \begin{matrix} & w_1 & w_2 \\ & [0.776 & 0.224] \end{matrix} & P'_1(V) &= \begin{matrix} & v_1 & v_2 & v_3 & v_4 \\ & [0.991 & 0.004 & 0.002 & 0.003] \end{matrix} \\
P'_1(U) &= \begin{matrix} & u_1 & u_2 & u_3 & u_4 & u_5 & u_6 & u_7 & u_8 & u_9 & u_{10} \\ & [0.733 & 0.017 & 0.013 & 0.01 & 0.002 & 0.036 & 0.126 & 0.011 & 0.018 & 0.034] \end{matrix} \\
P'_2(W) &= \begin{matrix} & w_1 & w_2 \\ & [0.285 & 0.715] \end{matrix} & P'_2(V) &= \begin{matrix} & v_1 & v_2 & v_3 & v_4 \\ & [0.143 & 0.035 & 0.463 & 0.359] \end{matrix} \\
P'_2(U) &= \begin{matrix} & u_1 & u_2 & u_3 & u_4 & u_5 & u_6 & u_7 & u_8 & u_9 & u_{10} \\ & [0.00018 & 0.109 & 0.004 & 0.69 & 0.003 & 0.00025 & 0.018 & 0.066 & 0.071 & 0.039] \end{matrix}
\end{aligned}$$

Fig. 7: Exogenous distributions in two different prior models.

In line 5 of Algorithm 2, the EM algorithm is executed with the previous prior distributions. After 500 iterations, the resulting distributions are those shown in Fig. 8. With these distributions, two fully-specified SCMs \mathcal{M}_1 and \mathcal{M}_2 are built. Both compose the set \mathcal{M} which is finally returned by Algorithm 2.

After the learning process, Algorithm 3 is used for bounding any causal or counterfactual query. Assume that our goal is to assess the necessity and sufficiency of

$$\begin{aligned}
P_1(W) &= \begin{matrix} w_1 & w_2 \\ [0.725 & 0.275] \end{matrix} & P_1(V) &= \begin{matrix} v_1 & v_2 & v_3 & v_4 \\ [0.552 & 0.012 & 0.207 & 0.229] \end{matrix} \\
P_1(U) &= \begin{matrix} u_1 & u_2 & u_3 & u_4 & u_5 & u_6 & u_7 & u_8 & u_9 & u_{10} \\ [0.183 & 0.03 & 0.014 & 0.042 & 0.011 & 0.029 & 0.354 & 0.103 & 0.036 & 0.198] \end{matrix} \\
P_2(W) &= \begin{matrix} w_1 & w_2 \\ [0.725 & 0.275] \end{matrix} & P_2(V) &= \begin{matrix} v_1 & v_2 & v_3 & v_4 \\ [0.469 & 0.094 & 0.289 & 0.148] \end{matrix} \\
P_2(U) &= \begin{matrix} u_1 & u_2 & u_3 & u_4 & u_5 & u_6 & u_7 & u_8 & u_9 & u_{10} \\ [0.001 & 0.264 & 0.001 & 0.013 & 0.0 & 0.025 & 0.277 & 0.132 & 0.264 & 0.023] \end{matrix}
\end{aligned}$$

Fig. 8: Exogenous distributions after running EM during 500 iterations.

immigration for agriculture. In this case, the counterfactual query of interest is PNS, defined as $P(A_{I=yes} = yes, A_{I=no} = no)$. Such query requires to build the counterfactual model displayed in Fig. 9 from each fully-specified SCM and then run the corresponding inference task. If this is done considering the previously mentioned models \mathcal{M}_1 and \mathcal{M}_2 , then the resulting PNS values are 0.058 and 0.228 respectively. From this, such counterfactual query can be bounded and it can be concluded that $PNS(I, A) \in [0.058, 0.228]$. Notice the low error achieved taking into account that the exact interval for this query is $[0.0, 0.243]$.

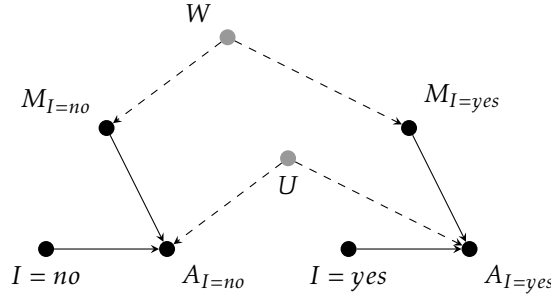


Fig. 9: Counterfactual model for computing the query $PNS(I, A)$.

4 Case of study

4.1 Problem and data description

To illustrate the potential of counterfactual reasoning with PGMs, let us consider the environmental data chosen for the case study, which is related to the region of Andalusia, in southern Spain (Fig. 10 (a)). This region shows high variability regarding elevation, ranging from 0 to 3460 m above the sea level. The main mountain ranges within the study area are the Sierra Morena mountain range in the North and

the Baetic Systems in the South, with the Baetic Depression serving as the geological boundary between them. The Guadalquivir River flows through this depression, being the largest river in Andalusia. The flattest areas correspond to the littoral and the Baetic depression, while the steepest ones correspond to the Baetic Systems. Therefore, Andalusia can be divided into 4 main geomorphological units: the Baetic Depression, the Sierra Morena mountain range, the Baetic Systems and the Littoral, as shown in Fig. 10 (b).

The Baetic Depression is characterized by its high agricultural production, mainly comprising rain-fed herbaceous crops in the low-lying plains and irrigated herbaceous crops along the Guadalquivir river (Fig. 10 (c)). The Sierra Morena mountain range is characterized by having high emigration and mortality rates and low birth rate, which results in population decline (Fig. 10 (d)), and is predominantly covered by rain-fed crops and dehesa, a heterogeneous system exhibiting various states of ecological maturity, with shepherding being the principal economic activity. The Baetic Systems have the highest elevation and steepness in the study area. This area is predominantly cloaked in natural vegetation, with extensive woody crops as a secondary feature. Its rugged terrain discourages the adoption of intensive agricultural practices. Finally, the Littoral, densely populated and characterized by high temperatures, features abundant natural vegetation and serves as the primary location for the majority of greenhouses in the study area, making it a focal point of agricultural activity.

In a previous study (Maldonado et al, 2018), 75 different variables representing social, economic and ecological characteristics of the study area were employed to construct an Object Oriented Bayesian network (OOBN), with no causal (nor counterfactual) reasoning conducted at that time. These variables, available in public repositories, were sourced from the Multi-territorial Information System of Andalusia (SIMA) and the Andalusian Environmental Information Network, and municipalities within the study area were taken as the modeling unit. Conversely, in our current study, we narrowed our focus to a subset of 17 variables from the original data-set, to conduct a causal analysis using SCMs. These include land-use, social, and economic variables which are detailed in Tables 2,3, and 4, respectively.

Table 2: Variables representing the ecological dimension used to construct the SCM.

Ecological dimension			
Name	Description	State	Threshold
MGU	The main geomorphological unit a municipality belongs to.	Baetic Depr. Sierra Morena Baetic Sys. Littoral	
Built	Percentage of artificial or built areas in each municipality - including <i>urban; industrial; mining; freight and technical infrastructures</i> .	Scarce Fair Abundant	< 5 5 - 30 > 30
GH	Percentage of intensive agriculture (greenhouses) in each municipality.	Scarce Fair Abundant	< 5 5 - 30 > 30
HCrops	Percentage of herbaceous crops in each municipality - including rainfed and irrigated crops.	Scarce Fair Dominant	< 15 15 - 50 > 50

Table 2: Variables representing the ecological dimension used to construct the SCM.

Ecological dimension			
Name	Description	State	Threshold
WCrops	Percentage of woody crops in each municipality - including rainfed and irrigated crops.	Scarce Fair Dominant	< 15 15 - 50 > 50
Mixed	Percentage of heterogeneous lands in each municipality - including patches mixing <i>grassland and forest and crops with natural vegetation</i> .	Scarce Fair Dominant	< 10 10 - 40 > 40
Natural	Percentage of natural areas in each municipality - comprising <i>bush; grassland; forest; bush and forest; wetlands and naked soil</i> .	Scarce Fair Dominant	< 25 25 - 60 > 60

Table 3: Variables representing the social dimension used to construct the SCM.

Social dimension			
Name	Description	State	Threshold
Pop	Population density of each municipality in 2011 (inhabitants/ Km^2).	Low Moderate High	< 35 35- 150 > 150
SR	Sex ratio. Proportion of males (M) to females (F) in each municipality in 2011 (computed as $SR = \frac{M}{M+F}$).	More females More males	≤ 0.50 > 0.50
EGR	Population growth rate. Exponential growth of the population, computed as $EGR = \frac{\ln(P_t/P_0)}{t}$, where P_0 represents the population in 2001, P_t the population in 2011 and t the 10-year period.	Decrease Stable Increase	< -0.03 -0.03 - 0.03 > 0.03
IME	Index of Migration effectiveness. Percentage of total migration for the period 2001-2011. It ranges from -100 (emigration) to 100 (immigration), with values close to 0 indicating no change in the population dynamic. It is computed as $IME = \frac{Immigration - Emigration}{Immigration + Emigration} \times 100$.	Emigration Balanced Immigration	< -2 -2 - 2 > 2
ODI	Old-age dependency index. Percentage of the older over the younger population in 2011, computed as $ODI = \frac{P_{>65}}{P_{<15}} \times 100$, where $P_{>65}$ is the population older than 65 years old and $P_{<15}$ is the population younger than 15 years old.	Low Moderate High	< 25 25 - 40 > 40
Death	Mortality rate. Number of deaths per 1000 inhabitants in each municipality in 2011.	Low Moderate High	< 9 9 - 15 > 15
Birth	Birth rate. Number of births per 1000 inhabitants in each municipality in 2011.	Low Moderate High	< 5.6 5.6 - 10.3 > 10.3

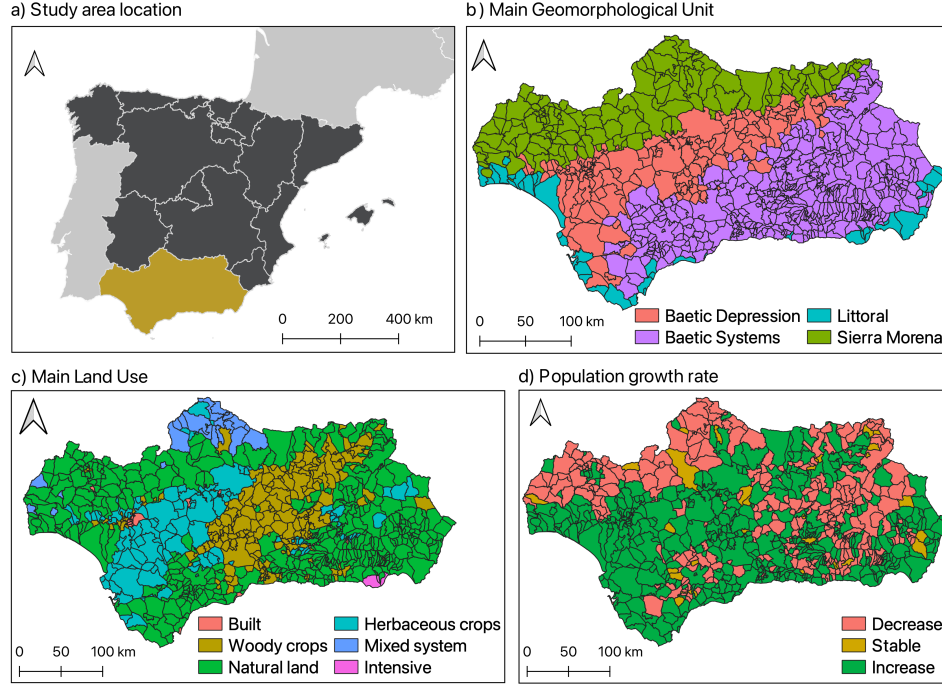


Fig. 10: Study area (Andalusia, Spain) (a) and municipalities within the study area, color-coded based on their primary geomorphological unit (b), their main land-use (c), and their population growth rate (d). For (b) and (c), in cases where a municipality encompasses more than one geomorphological unit or land-use, the color represents the larger or dominant one within that municipality.

Table 4: Variables representing the economic dimension used to construct the SCM.

Economic dimension			
Name	Description	State	Threshold
WF	Workforce. Percentage of the municipality's working age population (≥ 16) that are available to work in 2011. It is computed as $WF = \frac{ER+UR}{P_{\geq 16}} \times 100$; where ER is the Employment Rate; UR is the Unemployment Rate and $P_{\geq 16}$ is the population older than 16 years old.	Low Average High	< 0.55 $0.55 - 0.62$ > 0.62
SSE	Secondary sector employment. Number of employees in the secondary sector per 1000 inhabitants.	Low Moderate High	< 70 $70 - 113$ > 113
TSE	Tertiary sector employment. Number of employees in the trading, banking and service sectors per 1000 inhabitants.	Low Moderate High	< 78 $78 - 122$ > 122

The primary goal of this study is to investigate how different variables of interest in socioecological systems are influenced by other variables. In this context, such variables of interest are termed *effect variables*, while the other factors that could

potentially influence these effects are referred to as *cause variables*. In connection to Section 3.3, X and Y represent the cause and effect variables respectively. Specifically, we consider as effects those variables representing the different land uses and the population growth (i.e., *Built*, *GH*, *HCrops*, *WCrops*, *Mixed*, *Natural* and *EGR*). We will refer to *variables of interest* as the union of the cause and effect variable sets.

4.2 Data preprocessing and model definition

To conduct any causal or counterfactual analysis, it is necessary to define the cause and effect variables in such a way that their values can be categorized into two groups. In this case, since the variables are categorical (with multiple states), they are transformed into a binary format by collapsing their values into two distinct states: one representing a positive outcome and the other a negative outcome. Table 5 shows the partitions of the states considered for each variable in the dataset.

Table 5: Categorization into positive and negative values.

Variable	Positive state	Negative state
MGU	Littoral, Baetic Depression	Baetic System, Sierra Morena
Built	Abundant, Fair	Scarce
GH	Abundant, Fair	Scarce
Hcrops	Dominant, Fair	Scarce
Wcrops	Dominant, Fair	Scarce
Mixed	Dominant, Fair	Scarce
Natural	Dominant, Fair	Scarce
Pop	High	Low, Moderate
SR	More females	More males
EGR	Increase	Decrease, Stable
IME	Immigration	Emigration, Balanced
ODI	Low	Moderate, High
Death	Low	Moderate, High
Birth	High	Low, Moderate
WF	High	Low, Average
SSE	High	Low, Moderate
TSE	High	Low, Moderate

Given that the counterfactual analysis relies on SCMs, a causal structure in the form of a DAG is required. To establish this structure, we adopt the BN structure used in the aforementioned prior investigation (Maldonado et al, 2018), initially formulated by domain experts. Nonetheless, some modifications are made with the purpose of reducing its complexity, resulting in the graph shown in Fig. 11. First, the graph is restricted to our effect variables and their ancestors, i.e. the variables of interest previously detailed in Tables 2,3, and 4. Note that any descendant from the effect variables in the original graph is irrelevant for a causal analysis. Additionally, the node *MGU* is a common ancestor of all the cause and effect variables considered, and there exists no alternative path connecting them with the ancestors excluded from the final graph. Consequently, our variables of interest are independent from the rest of ancestors given *MGU*. Secondly, the number of parents is limited to a maximum of three. The intention of this is to prevent extremely large exogenous

variables, whose number of states increases exponentially with the number of parents. Hence, the arc from *MGU* to *Pop* is removed. Note that there are alternative directed paths between both nodes, i.e., it is redundant. Moreover, this deletion is the one involving the lowest decrease in the likelihood of the model given the data.

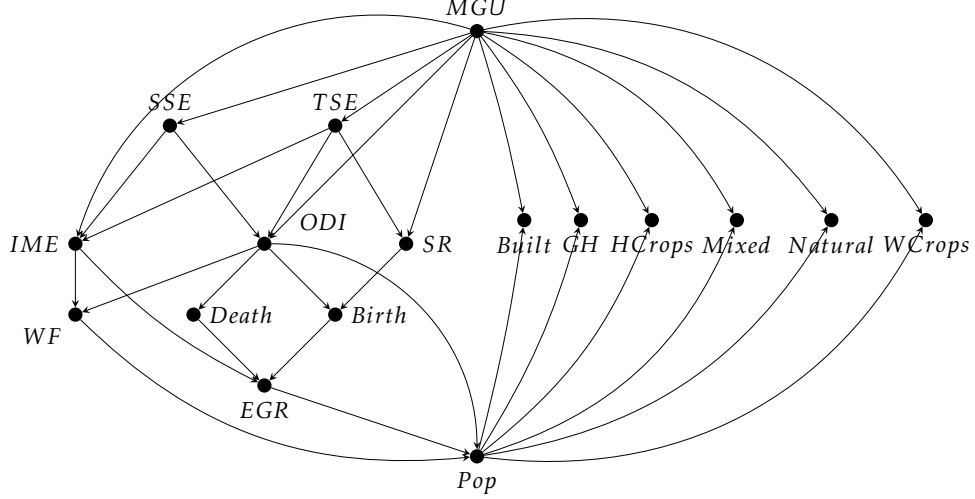


Fig. 11: BN obtained from the model in a previous study (Maldonado et al, 2018) by restricting it to our variables of interest and by limiting the number of parents to 3.

After establishing the causal structure, a SCM can be derived by introducing an exogenous parent for each endogenous variable. The resulting graph is illustrated in Fig. 12. As for the parameters, the SEs are defined in a canonical form and constructed using Algorithm 1. By contrast, the marginal distributions over the exogenous variables are considered to be unknown and estimated using EMCC (i.e., Algorithm 2). Specifically, this method is executed with 100 EM runs ($N = 100$) while capping the EM convergence at 300 iterations.

Using Algorithm 3, we compute various queries in our case study. Initially, we examine the difference in conditional probability, denoted as $P(y|x) - P(y|x')$. This aligns with the conventional BN analysis. Moving to causal (non-counterfactual) reasoning, we investigate the interventional query ACE, defined in Eq. (13). To underscore the advantages of counterfactual reasoning, we evaluate the queries PN, PNrc, PS, and PNS, outlined in eqs. (6) to (9). The variables under study (i.e., effects) are those enumerated in the preceding section, while the causes vary based on the specific effect. This distinction arises from the requirement that causes must be ancestors of the effects. In this sense, in the case of land use variables, the causes include *WF*, *EGR*, *MGU*, *SR*, *SSE*, *TSE*, *ODI*, *Pop*, *Death*, and *Birth*. When *EGR* is treated as the effect, *Pop* and the variable itself are excluded as potential causes.

In relation to the implementation, the CREDICI software (Cabañas et al, 2020) is used, a Java library designed for causal reasoning, featuring the implementation

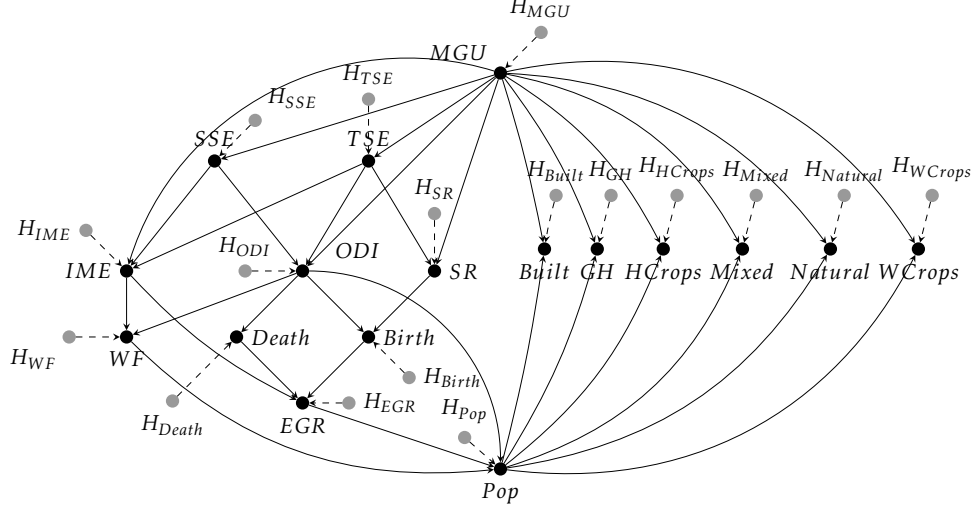


Fig. 12: Markovian SCM used for intended counterfactual analysis. All the SEs are assumed to be canonical.

of EMCC. For more extensive implementation details and the code to replicate these experiments, please refer to our GitHub repository².

5 Results and discussion

To begin with the analysis of the results, we first consider as *effect* the variable *EGR* (population growth rate), whose results are given in Fig. 13. The variable with a clearer causal impact on *EGR* is *IME*. Remarkably, the probability of sufficiency, PS is bounded between 0.73 and 0.85, which means that it is very probable that a positive value of *IME* (immigration) is enough to produce a positive value of *EGR* (increase) despite the values of the other variables. Besides, it is also quite likely that *IME* is a necessary condition for *EGR* to have a high value, since $PN(IME, EGR) \in [0.60, 0.75]$. The probability of necessity and sufficiency is also bounded above 0.5, more precisely in the interval $[0.51, 0.63]$. Regarding the other variables under consideration, *MGU* and *TSE* are likely to be sufficient for *EGR* to take place, reaching values in the intervals $[0.54, 0.78]$ and $[0.63, 0.82]$ respectively. Conversely, *SSE*, *ODI*, *Death* and *Birth* have a good chance to be sufficient, since their lower bounds are close to 0.4.

With respect to non-counterfactual queries, the difference in conditional probability (0.58) and the average causal effect in the interval $[0.50, 0.56]$ support the classification of positive *IME* as a cause of positive *EGR*. It is important to note that while non-counterfactual queries enable the identification of variables influencing *EGR*, these queries do not provide information about the nature of the relationship (whether it is one of necessity or sufficiency). This limitation underscores the

²<https://github.com/PGM-Lab/2023-counterfactual-land>

nuanced insights that counterfactual reasoning can offer in understanding causal relationships within the studied context.

Therefore, a positive immigration rate turns out to be both necessary and sufficient (with high probability) in order to achieve a positive population growth rate (Parsons and Smeeding, 2006; Viñuela et al, 2019; Viñuela, 2022). On the other hand, it is also likely that the location of the municipality and the tertiary sector employment can cause a positive *EGR* value, but this is only expressed in terms of sufficiency. As a matter of fact, Figure 10 (d) indicates a population decline in the majority of municipalities situated in both the Baetic Systems and Sierra Morena regions. Considering the remaining causes, population growth can occur in the absence of all of them, though they might be sufficient on their own to drive population growth. Population growth is a phenomenon influenced by various factors, including immigration, emigration, death, and birth rates (Lutz, 2006; Poston Jr and Bouvier, 2010). The variable *IME* is an index that incorporates both immigration and emigration rates. A high value of *IME* indicates more immigration than emigration, resulting in population increase, assuming that other factors remain constant. In contrast, death and birth rates are considered separately rather than jointly in a single rate of natural population increase. Individually, neither low death rate nor high birth rate is necessary, for population growth. However, if both were considered as such index, its probability of necessity could be higher.

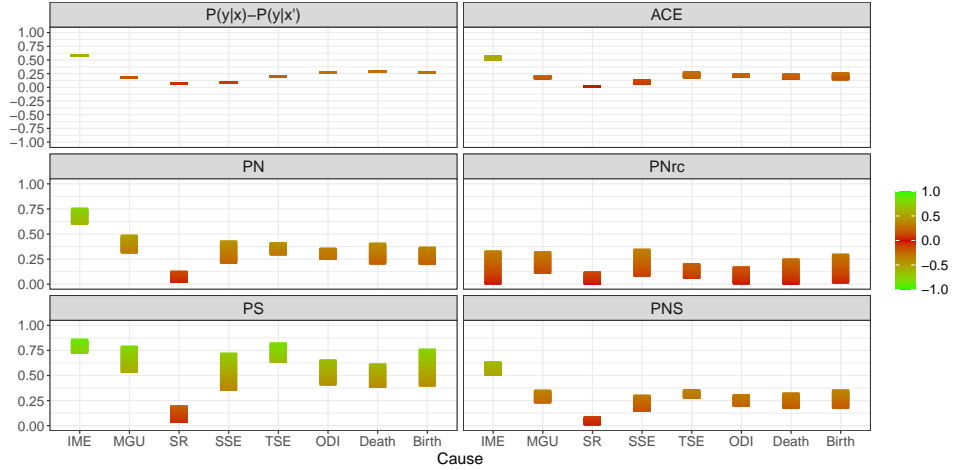


Fig. 13: Intervals for the queries with *EGR* as effect variable.

The remaining *effect* variables are all referred to land uses. For variable *Built* which represents the percentage of built or artificial areas in a municipality, only two variables turn out to have a significant causal effect, namely the location of the municipality, *MGU* and its population density, *Pop*. It is no wonder that *Pop* is the most clear sufficient cause of positive value of *Built*, with $PS(Pop, Built) > 0.93$. However, the probability of necessity for this variable is lower, but still remarkable,

between 0.65 and 0.70. The same probability reaches higher values for the location of the municipality, reaching the interval $[0.62, 0.82]$. Nonetheless, the probability of sufficiency of *MGU* is in $[0.55, 0.73]$, which is notably lower than that for the other variable. Moreover, both causes have a good chance of being necessary and sufficient for *Built* to be abundant or fairly abundant. Hence, the results of the queries seem to indicate that the location (flat vs. mountainous areas) is fundamental when determining the percentage of built area, but also in combination with the population density (Ehrlich et al, 2021; Thornton et al, 2022).

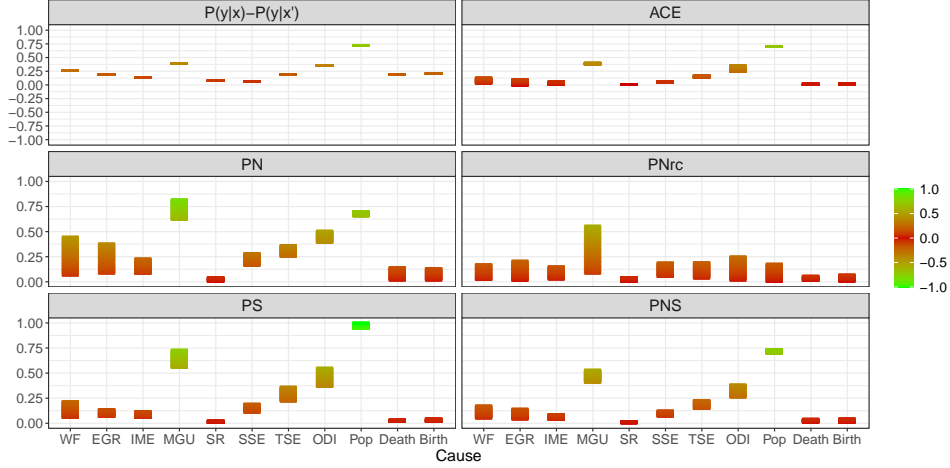


Fig. 14: Intervals for the queries with *Built* as effect variable.

Fig. 15 shows the results of the queries related to variable *HCrops*, which is the percentage of herbaceous crops in the municipality. In this case, only variable *MGU* reaches a value clearly above 0.5, and only for one query, the probability of necessity, which is estimated to be in the interval $[0.59, 0.99]$. It means that it is quite likely that a positive value of *MGU* (littoral, Baetic depression) is necessary for a positive value of *HCrops* (dominant, fair) to be observed, but it is not so clearly rendered as sufficient too, since $PS(MGU, HCrops) \in [0.44, 0.74]$, however there is still some chance that it is sufficient. On the other hand, *WF* and *Pop* show a high uncertainty with respect to the probability of necessity, since their intervals are considerably wide. The remaining variables are clearly not necessary, nor sufficient, for *HCrops*. The findings align coherently with the insights derived from Figure 10 (c). Herbaceous crops emerge as the predominant land use across a significant portion of the Baetic Depression, whereas they do not hold the same prevalence in other geomorphological units (Molero and Marfil, 2017).

In the case of the percentage of greenhouses (variable *GH*), the results are displayed in Fig. 16. It is apparent from the plots that only three variables, *MGU*, *Pop* and *ODI*, have a causal impact on the target variable *GH*. The most remarkable

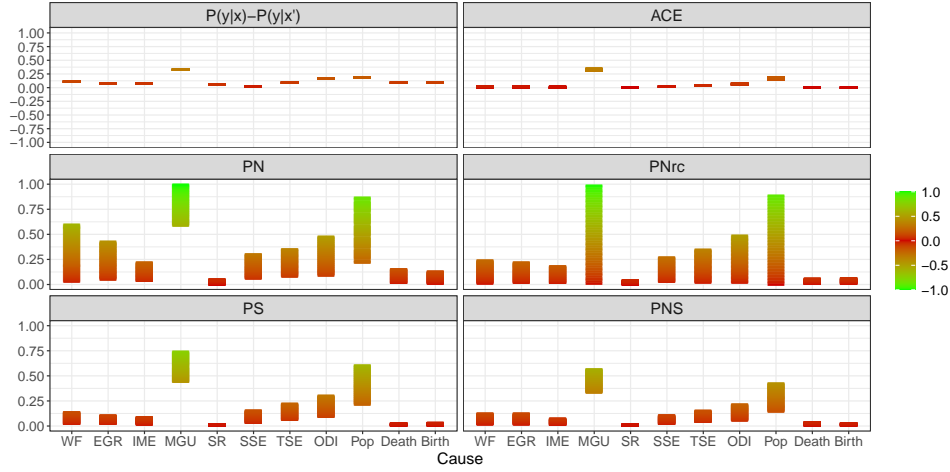


Fig. 15: Intervals for the queries with *HCrops* as effect variable.

effect is observed in terms of the probability of necessity, with values in the intervals $[0.72, 1]$, $[0.88, 1]$ and $[0.69, 0.91]$ for *MGU*, *Pop* and *ODI*, respectively, which indicates that it is considered almost certain that all three variables must have a positive value for *GH* to have a positive value as well (Aznar-Sánchez et al, 2011; Mendoza-Fernández et al, 2021). In addition, variable *TSE*, with the upper bound for PN above 0.5 and the lower one close to 0.5, has a good chance to be necessary (Galdeano-Gómez et al, 2013). It is also quite significant that none of the variables is sufficient condition by its own. With respect to the non-counterfactual queries, none of the insights previously mentioned are reflected in such queries, which showcases the advantage of counterfactual reasoning. The results coherently reflect the predominant location of greenhouses in the Littoral (Figure 10 (c)). However, it is important to note that the positive state of *MGU* encompasses both the Littoral and the Baetic Depression, with the latter not exhibiting a notably high density of greenhouses. Therefore, *MGU* is necessary but not sufficient condition for *GH* (Wolosin, 2008).

The results for variable *Natural*, representing the percentage of natural areas, can be seen in Fig. 17. In terms of the difference in conditional probability and average causal effect, only the location (*MGU*) shows a remarkable variation. Regarding the probability of necessity, all variables except *MGU* and *Pop* are very unlikely to be necessary, due to the low value of the upper bounds of their intervals. Even the two mentioned variables are not clearly necessary, since most of their intervals are below 0.5, and their widths indicate uncertainty about the probability value. It is also clear that all variables except *MGU* and *Pop* are very unlikely to be sufficient to increase the natural spaces. The intervals for *MGU* and *Pop* are compatible with them being sufficient conditions, but their amplitude indicate that there is considerable uncertainty. The most remarkable insight about the natural areas can be obtained from the high value in the query PNrc with *MGU* as cause variable. This shows that not being in the littoral nor in the Baetic depression is necessary to have mainly a natural land

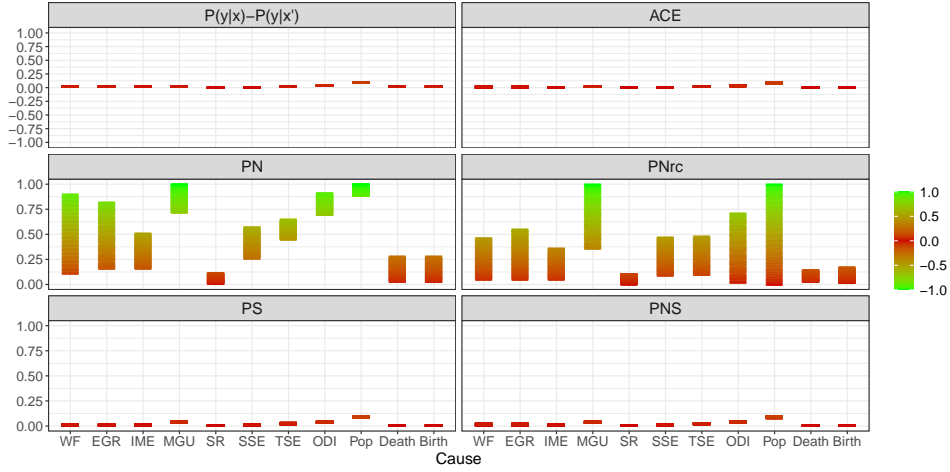


Fig. 16: Intervals for the queries with *GH* as effect variable.

use, since $PNrc(MGU, Natural) \in [0.67, 0.87]$. In other words, mountainous areas (Sierra Morena and Baetic Systems) are necessary for the natural areas to be dominant over the other land uses. The results align with the fact that natural lands are predominantly located in the Baetic Systems and Sierra Morena mountain ranges, as shown in Figure 10 (c) (Gratzner and Keeton, 2017; Snethlage et al, 2022).

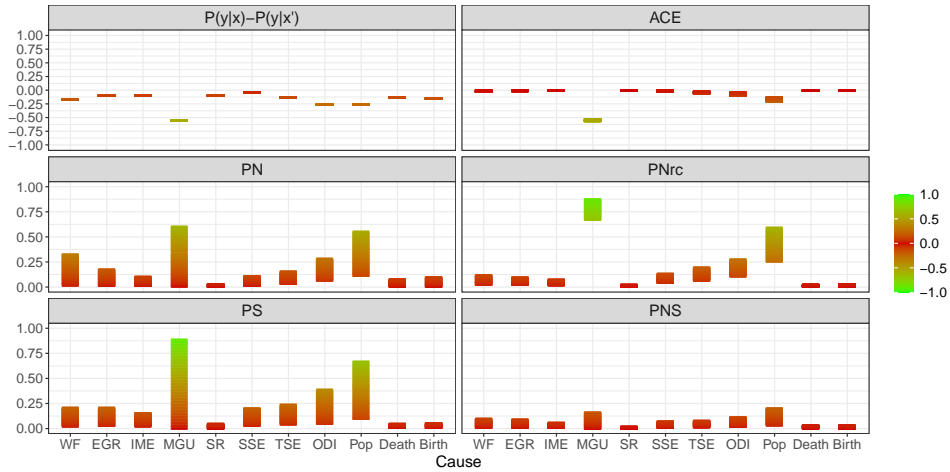


Fig. 17: Intervals for the queries with *Natural* as effect variable.

Fig. 18 shows the results for variable *WCrops*, which measures the percentage of woody crops in each municipality. It can be seen that none of the variables shows a significant variation in conditional probability or remarkable values of ACE. Considering the queries related to necessity and sufficiency, *MGU* and *Pop* might have a

significant influence on *WCrops*, but the width of the corresponding intervals poses a high level of uncertainty on such statement. The rest of possible causes are clearly not relevant.

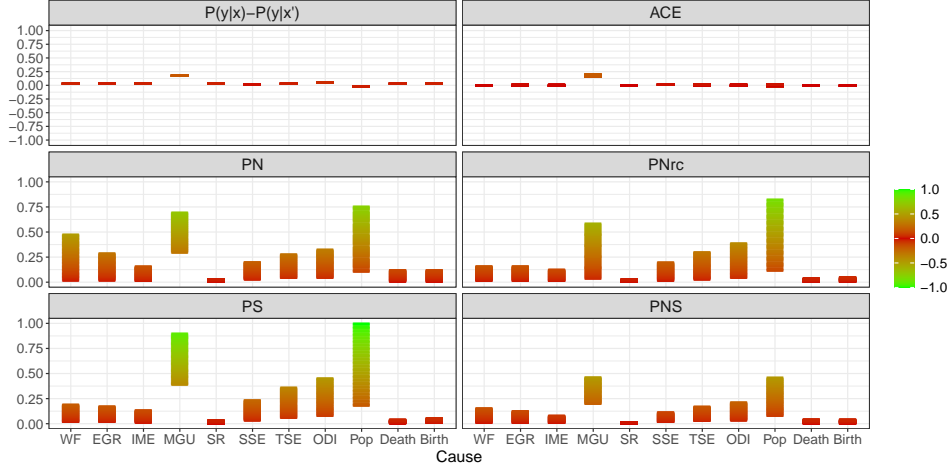


Fig. 18: Intervals for the queries with *WCrops* as effect variable.

Finally, Fig. 19 displays the results for variable *Mixed* (percentage of heterogeneous lands). The only causal effect in terms of difference in conditional probability and ACE is provided by variables *Pop* and *MGU*. It is highly unlikely that all variables except *MGU* and *Pop* are necessary (see PN, PNS and PNrc), but even for these two variables there is paramount uncertainty in terms of PN. However, PNrc clearly points towards the facts that not being in the littoral nor in the Baetic depression and having a low population density are both necessary conditions. On the other hand, the values of PS and PNS clearly show that none of the variables are sufficient for *Mixed* to have a positive value. The results are consistent with the fact that heterogeneous lands are the main land-use in some areas of Sierra Morena (Muñoz-Rojas et al, 2011; Plieninger et al, 2021), coinciding with a concurrent trend of population decline in those regions, as shown in Figure 10 (c,d) (Plieninger and Wilbrand, 2001).

6 Conclusions

This paper has proposed an application of counterfactual reasoning with PGMs to analyze socioecological systems. This approach addresses a limitation in traditional probabilistic analysis, where despite the ability to identify influences between variables, the nature of the relationship cannot be determined (whether it is one of necessity or sufficiency). For the counterfactual analysis, a recently developed technique is suggested, working specifically with PGMs for causal and counterfactual reasoning. An advantage of this method is its capability to calculate bounds for certain queries termed as unidentifiable, a task challenging for other similar

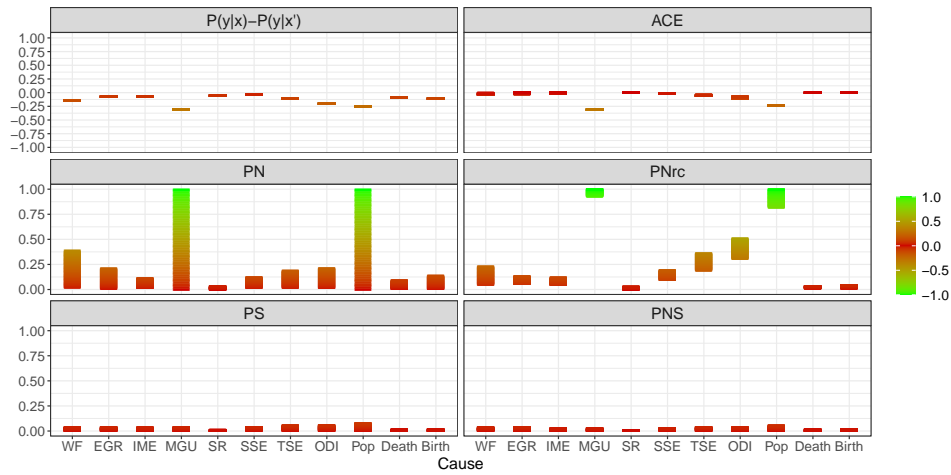


Fig. 19: Intervals for the queries with *Mixed* as effect variable.

methods. Notably, this is achieved through the analysis of observational data alone, distinguishing it from other methods that additionally require interventional data.

To demonstrate the efficacy of counterfactual reasoning, we have presented a case study using an observational data-set containing information on socioeconomic factors and land uses in various areas in southern Spain. The primary conclusion drawn from this study is that both the location and population density are essential for most land uses. Specifically, a mountainous location with low population density is deemed necessary for natural or mixed land uses. Conversely, a non-mountainous location with high population density is required for the presence of built areas, herbaceous crops, or greenhouses. Concerning population growth, our study indicates that immigration is not only necessary but also a sufficient condition for population increase. All these findings underscores the power of counterfactual reasoning in uncovering relationships within socioecological systems.

While this study provides valuable insights, additional research could be carried out to consider counterfactual queries with multiple cause variables, for instance to determine whether simultaneous causes are jointly sufficient. Additionally, this methodology could be of considerable interest for other topics within the environmental and ecological areas, such as the study of species distribution or risk assessments.

Declarations

Funding. This research is part of projects PID2019-106758GB-C32 and PID2022-139293NB-C31, funded by MCIN/AEI/10.13039/501100011033, FEDER funds. R.C. was also funded by the “María Zambrano” grant (RR_C_2021_01) from the Spanish Ministry of Universities and funded with NextGenerationEU funds. A.D.M. acknowledges the support by Junta de Andalucía through Grant DOC.00358.

Conflict of interest. The authors have no relevant financial or non-financial interests to disclose.

Code and data availability. The code and data-set used in the current study is available at <https://github.com/PGM-Lab/2023-counterfactual-land>.

Authors' contributions. Conceptualization, R.C., A.D.M and P.A.A.; methodology and software, R.C. and M.M.; results analysis, R.C., A.D.M. and A.S.; writing–original draft preparation, R.C., A.D.M, M.M., P.A.A. and A.S.; funding acquisition, A.S.; supervision, P.A.A. and A.S. All authors have read and agreed to the published version of the manuscript.

References

- Andam KS, Ferraro PJ, Pfaff A, et al (2008) Measuring the effectiveness of protected area networks in reducing deforestation. *Proceedings of the national academy of sciences* 105(42):16089–16094
- Anderies JM, Janssen MA, Ostrom E (2004) A framework to analyze the robustness of social-ecological systems from an institutional perspective. *Ecology and Society* 9(1):18. URL <http://www.ecologyandsociety.org/vol9/iss1/art18/>
- Arnaiz-Schmitz C, Aguilera PA, Ropero RF, et al (2023) Detecting social-ecological resilience thresholds of cultural landscapes along an urban–rural gradient: a methodological approach based on bayesian networks. *Landscape Ecology* <https://doi.org/10.1007/s10980-023-01732-9>
- Avin C, Shpitser I, Pearl J (2005) Identifiability of path-specific effects. In: *IJCAI International Joint Conference on Artificial Intelligence*, pp 357–363
- Aznar-Sánchez JA, Galdeano-Gómez E, Pérez-Mesa JC (2011) Intensive horticulture in almería (spain): A counterpoint to current european rural policy strategies. *Journal of Agrarian Change* 11(2):241–261
- Bareinboim E, Correa JD, Ibeling D, et al (2022) On pearl’s hierarchy and the foundations of causal inference. In: *Probabilistic and causal inference: the works of judea pearl*. ACM, p 507–556
- Berkes F, Colding J, Folke C (2003) *Navigating social-ecological systems: Building resilience for complexity and change*. Cambridge University Press, Cambridge, UK
- Biggs R, Rhode C, Archibald S, et al (2015) Strategies for managing complex social-ecological systems in the face of uncertainty: examples from south africa and beyond. *Ecology and Society* 20(1):52. <https://doi.org/10.5751/ES-07380-200152>
- Bizzi S, Surridge BW, Lerner DN (2013) Structural equation modelling: a novel statistical framework for exploring the spatial distribution of benthic macroinvertebrates in riverine ecosystems. *River Research and Applications* 29(6):743–759

- Cabañas R, Antonucci A, Huber D, et al (2020) Credici: a java library for causal inference by credal networks. In: International Conference on Probabilistic Graphical Models, PMLR, pp 597–600
- Carriger JF, Barron MG (2011) Minimizing risks from spilled oil to ecosystem services using influence diagrams: The deepwater horizon spill response. *Environmental science & technology* 45(18):7631–7639
- Carriger JF, Newman MC (2012) Influence diagrams as decision-making tools for pesticide risk management. *Integrated environmental assessment and management* 8(2):339–350
- Carriger JF, Barron MG, Newman MC (2016) Bayesian networks improve causal environmental assessments for evidence-based policy. *Environmental science & technology* 50(24):13195–13205
- Correa J, Lee S, Bareinboim E (2021) Nested counterfactual identification from arbitrary surrogate experiments. *Advances in Neural Information Processing Systems* 34:6856–6867
- De Aranzabal I, Schmitz MF, Aguilera P, et al (2008) Modelling of landscape changes derived from the dynamics of socio-ecological systems: A case of study in a semiarid mediterranean landscape. *Ecological Indicators* 8:672–685
- Ehrlich D, Melchiorri M, Capitani C (2021) Population trends and urbanisation in mountain ranges of the world. *Land* 10(3):255
- Ferraro PJ (2009) Counterfactual thinking and impact evaluation in environmental policy. *New directions for evaluation* 2009(122):75–84
- Galdeano-Gómez E, Aznar-Sánchez JA, Pérez-Mesa JC (2013) Sustainability dimensions related to agricultural-based development: the experience of 50 years of intensive farming in almería (spain). *International Journal of Agricultural Sustainability* 11(2):125–143
- Gratzer G, Keeton WS (2017) Mountain forests and sustainable development: The potential for achieving the united nations’ 2030 agenda. *Mountain research and development* 37(3):246–253
- Hatami R (2018a) Development of a protocol for environmental impact studies using causal modelling. *Water research* 138:206–223
- Hatami R (2018b) A practical method to control spatiotemporal confounding in environmental impact studies. *MethodsX* 5:710–716
- Hatami R (2019) A review of the techniques used to control confounding bias and how spatiotemporal variation can be controlled in environmental impact studies.

- Huang Y, Valtorta M (2006) Identifiability in causal bayesian networks: A sound and complete algorithm. In: Proceedings of the national conference on artificial intelligence, Menlo Park, CA; Cambridge, MA; London; AAAI Press; MIT Press; 1999, p 1149
- Hughes TP, Carpenter SR, Rockström J, et al (2013) Multiscale regime shifts and planetary boundaries. *Trends in Ecology & Evolution* 28(7):389–395. <https://doi.org/10.1016/J.TREE.2013.05.019>
- Irvine KM, Gitelman AI (2011) Graphical spatial models: a new view on interpreting spatial pattern. *Environmental and Ecological Statistics* 18:447–469. <https://doi.org/10.1007/s10651-010-0146-8>
- Irvine KM, Miller SW, Al-Chokhachy RK, et al (2015) Empirical evaluation of the conceptual model underpinning a regional aquatic long-term monitoring program using causal modelling. *Ecological indicators* 50:8–23
- Jensen FV, Nielsen TD (2007) Bayesian networks and decision graphs, vol 2. Springer, New York, NY
- Koller D, Friedman N (2009) Probabilistic graphical models: principles and techniques. MIT press, Cambridge, Massachusetts
- Lutz W (2006) Fertility rates and future population trends: will europe's birth rate recover or continue to decline? *International journal of andrology* 29(1):25–33
- Maldonado AD, Aguilera PA, Salmerón A, et al (2018) Probabilistic modeling of the relationship between socioeconomy and ecosystem services in cultural landscapes. *Ecosystems Services* 33:146–164
- Mathias J, Anderies J, Baggio J, et al (2020) Exploring non-linear transition pathways in social-ecological systems. *Scientific Reports* 10:4136. <https://doi.org/10.1038/s41598-020-59713-w>
- McConnachie MM, van Wilgen BW, Ferraro PJ, et al (2016) Using counterfactuals to evaluate the cost-effectiveness of controlling biological invasions. *Ecological Applications* 26(2):475–483
- Mendoza-Fernández AJ, Peña-Fernández A, Molina L, et al (2021) The role of technology in greenhouse agriculture: Towards a sustainable intensification in campo de dalías (almería, spain). *Agronomy* 11(1):101
- Molero J, Marfil JM (2017) Betic and southwest andalusia. *The Vegetation of the Iberian Peninsula: Volume 2* pp 143–247

- Muñoz-Rojas M, De la Rosa D, Zavala L, et al (2011) Changes in land cover and vegetation carbon stocks in andalusia, southern spain (1956–2007). *Science of the total environment* 409(14):2796–2806
- Nyberg JB, Marcot BG, Sulyma R (2006) Using Bayesian belief networks in adaptive management. *Canadian Journal of Forest Research* 36(12):3104–3116
- Parrott L, Quinn N (2016) A complex systems approach for multiobjective water quality regulation on managed wetland landscapes. *Ecosphere* 7(6):e01363
- Parsons CA, Smeeding TM (2006) *Immigration and the Transformation of Europe*. Cambridge University Press
- Paul WL (2011) A causal modelling approach to spatial and temporal confounding in environmental impact studies. *Environmetrics* 22(5):626–638
- Paul WL, Anderson MJ (2013) Causal modeling with multivariate species data. *Journal of Experimental Marine Biology and Ecology* 448:72–84
- Paul WL, Rokahr PA, Webb JM, et al (2016) Causal modelling applied to the risk assessment of a wastewater discharge. *Environmental monitoring and assessment* 188:1–20
- Pearl J (1988) *Probabilistic reasoning in intelligent systems*. Morgan-Kaufmann, San Mateo, CA
- Pearl J (2009) *Causality. Models, inference and reasoning*. Second edition. Cambridge University Press, New York
- Plieninger T, Wilbrand C (2001) Land use, biodiversity conservation, and rural development in the dehesas of cuatro lugares, spain. *Agroforestry Systems* 51:23–34
- Plieninger T, Flinzberger L, Hetman M, et al (2021) Dehesas as high nature value farming systems: a social-ecological synthesis of drivers, pressures, state, impacts, and responses. *Ecology and Society* 26(3):23
- Poston Jr DL, Bouvier LF (2010) *Population and society: An introduction to demography*. Cambridge University Press
- Preise R, Biggs R, Vos AD, et al (2018) Social-ecological systems as complex adaptive systems: organizing principles for advancing research methods and approaches. *Ecology and Society* 23(4):46. <https://doi.org/10.5751/ES-10558-230446>
- Punzo G, Castellano R, Bruno E (2022) Exploring land use determinants in italian municipalities: comparison of spatial econometric models. *Environmental and Ecological Statistics* 29:727–753. <https://doi.org/10.1007/s10651-022-00541-8>

- Ramazi P, Kunegel-Lion M, Greiner R, et al (2021) Exploiting the full potential of bayesian networks in predictive ecology. *Methods in Ecology and Evolution* 12(1):135–149
- Ropero RF, Rumí R, Aguilera PA (2019) Modelling relationships between socioeconomy, landscape and water flows in mediterranean agroecosystems: a case study in adra catchment (spain) using bayesian networks. *Environmental and Ecological Statistics* 26:47–86. <https://doi.org/10.1007/s10651-019-00419-2>
- Scheffer M, Carpenter S, Lenton T, et al (2012) Anticipating critical transitions. *Science* 338(6105):344–348. <https://doi.org/10.1126/science.1225244>
- Schmitz MF, De Aranzabal I, Aguilera PA, et al (2003) Relationship between landscape typology and socioeconomic structure: Scenarios of change in spanish cultural landscapes. *Ecological Modelling* 168:343–356
- Snethlage MA, Geschke J, Ranipeta A, et al (2022) A hierarchical inventory of the world’s mountains for global comparative mountain science. *Scientific data* 9(1):149
- Subramaniam Y, Masron TA, Loganathan N (2023) The impacts of migrants on environmental degradation in developing countries. *Environmental and Ecological Statistics* 30:17–40. <https://doi.org/10.1007/s10651-022-00552-5>
- Thornton JM, Snethlage MA, Sayre R, et al (2022) Human populations in the world’s mountains: Spatio-temporal patterns and potential controls. *Plos one* 17(7):e0271466
- Tian J, Pearl J (2000) Probabilities of causation: Bounds and identification. *Annals of Mathematics and Artificial Intelligence* 28(1-4):287–313
- Tian J, Pearl J (2002) A general identification condition for causal effects. In: *Aaai/iaai*, pp 567–573
- Viñuela A (2022) Immigrants’ spatial concentration: Region or locality attractiveness? *Population, Space and Place* 28(2):e2530
- Viñuela A, Gutierrez Posada D, Rubiera Morollon F (2019) Determinants of immigrants’ concentration at local level in spain: Why size and position still matter. *Population, Space and Place* 25(7):e2247
- Wolosin RT (2008) El milagro de almeria, españa: a political ecology of landscape change and greenhouse agriculture. PhD thesis
- Wu Y, Zhang L, Wu X (2019) Counterfactual fairness: Unidentification, bound and algorithm. In: *Proceedings of the twenty-eighth international joint conference on Artificial Intelligence*

- Zaffalon M, Antonucci A, Cabañas R (2020) Structural causal models are (solvable by) credal networks. In: International Conference on Probabilistic Graphical Models, PMLR, pp 581–592
- Zaffalon M, Antonucci A, Cabañas R, et al (2023a) Approximating counterfactual bounds while fusing observational, biased and randomised data sources. *International Journal of Approximate Reasoning* 162:109023
- Zaffalon M, Antonucci A, Cabañas R, et al (2023b) Efficient computation of counterfactual bounds. arXiv preprint arXiv:230708304